Journal of Alloys and Compounds 526 (2012) 53–58

Contents lists available at SciVerse ScienceDirect

Journal of Alloys and Compounds

journal homepage: www.elsevier.com/locate/jallcom

Large-scale synthesis of silicon arrays of nanowire on titanium substrate as high-performance anode of Li-ion batteries

Ning Du, Hui Zhang, Xing Fan, Jingxue Yu, Deren Yang*

State Key Lab of Silicon Materials and Department of Materials Science and Engineering, Zhejiang University, Hangzhou 310027, People's Republic of China

ARTICLE INFO

Article history:
Received 22 November 2011
Received in revised form 14 February 2012
Accepted 17 February 2012
Available online xxx

Keywords:
Silicon nanowires
Arrays
Titanium substrate
Li-ion batteries
Anode

ABSTRACT

We have demonstrated large-scale synthesis of Si nanowire arrays (SiNA) on Ti substrate and their application as high-performance anode of Li-ion batteries. SiNA were controllably synthesized through hot-filament chemical vapour deposition (HFCVD) using Au films of different thickness as a catalyst. We found that the thickness of the Au film based catalysts played important role in controlling the morphology of Si nanostructures. The thick Au layer (e.g., 50 nm) resulted in the formation of the SiNA, while the thin Au layer (e.g., 5 nm) led to the disordered Si nanowires. The as-synthesized SiNA exhibited large reversible capacity (3600 mAh g^{-1}) and high initial Coulombic efficiency (86.4%), which is much better than the disordered Si nanowires. The good contact and adhesion of SiNA with current collectors, as well as excellent strain accommodation might be responsible for the enhanced performance as anode of Li-ion batteries.

1. Introduction

Rechargeable lithium-ion batteries have been considered as an irreplaceable power storage for mobile devices and electric vehicles. However, the lithium storage capacity of commercial graphite was limited to the theoretical maximum capacity of 372 mAh g^{-1}, which could not satisfy the requirements for more and more developed applications [1]. Silicon (Si) has high theoretic capacity (about 4200 mAh g^{-1}) and relatively low working potential (0.5 V vs. Li/Li^+) [2–4], which has been considered as promising candidates compared to tin and transition oxide etc. However, Li alloying in Si was known to induce the formation of new intermetallic phases, leading to inhomogeneous volume expansions in the two-phase regions, and then cracking and finally pulverization of the materials [5,6]. As a consequence of this cracking, there is a loss of electrical contact between inter-particles as well as a resulted significant capacity decline. The use of Si nanostructures (e.g., nanoparticles, nanowires and nanotubes) is a popular approach to partially solve the aforementioned issues [7–19]. However, it was found that the nanostructured Si still suffered from interfacial kinetic problems, which originated from the assembled processes of batteries such as mixing with binder and carbon black, and patternmaking onto electrode substrates [7–19]. The interfacial problems would become more prominent during the charge–discharge process of the nanostructured Si, which also degraded the performance of Li-ion batteries.

A new class of electrodes based on nanoarrays grown directly on current collector has shown significant improvements in recent years by taking advantages of good contact and adhesion with current collectors, as well as excellent strain accommodation [20–30]. To this end, Martin and co-workers pioneered the porous membranes-assisted synthesis of nanowire arrays made of TiS_2, C, $LiMn_2O_4$ and so forth, which was applied as anode and cathode of Li-ion batteries [20–26]. Taberna and co-workers reported the synthesis of core–shell nanowires by electrochemical deposition of Fe_3O_4 on the surface of metal nanowires, which exhibited high-rate capacity as anode of Li-ion batteries [27,28]. Co_3O_4, SnO_2 and other arrays of nanowires were also synthesized directly onto the current collector via simple solution-based methods, which showed the improved performance in comparison with the corresponding disordered nanorods [29–32]. Most recently, Cui and co-workers have reported the synthesis of Si nanowires grown directly on the current collector as anode of Li-ion batteries [33]. The Si nanowires were synthesized through a vapour–liquid–solid (VLS) process on stainless steel substrates with Au film as a catalyst. The theoretic charge capacity for Si nanowires anodes was achieved and a discharge capacity close to 75% of this maximum was maintained with little fading during cycling. Nevertheless, various efforts should be employed to synthesize the SiNA in high-quality and yield for further upgrading the performance of Li-ion batteries.

Herein, we demonstrated the large-scale synthesis of the high-quality SiNA on titanium (Ti) substrates via hot-filament chemical vapour deposition (HFCVD) using Au film as a catalyst. It was

* Corresponding author. Tel.: +86 571 87953190; fax: +86 571 87952322.
E-mail address: mseyang@zju.edu.cn (D. Yang).

0925-8388/$ – see front matter © 2012 Elsevier B.V. All rights reserved.
doi:10.1016/j.jallcom.2012.02.109

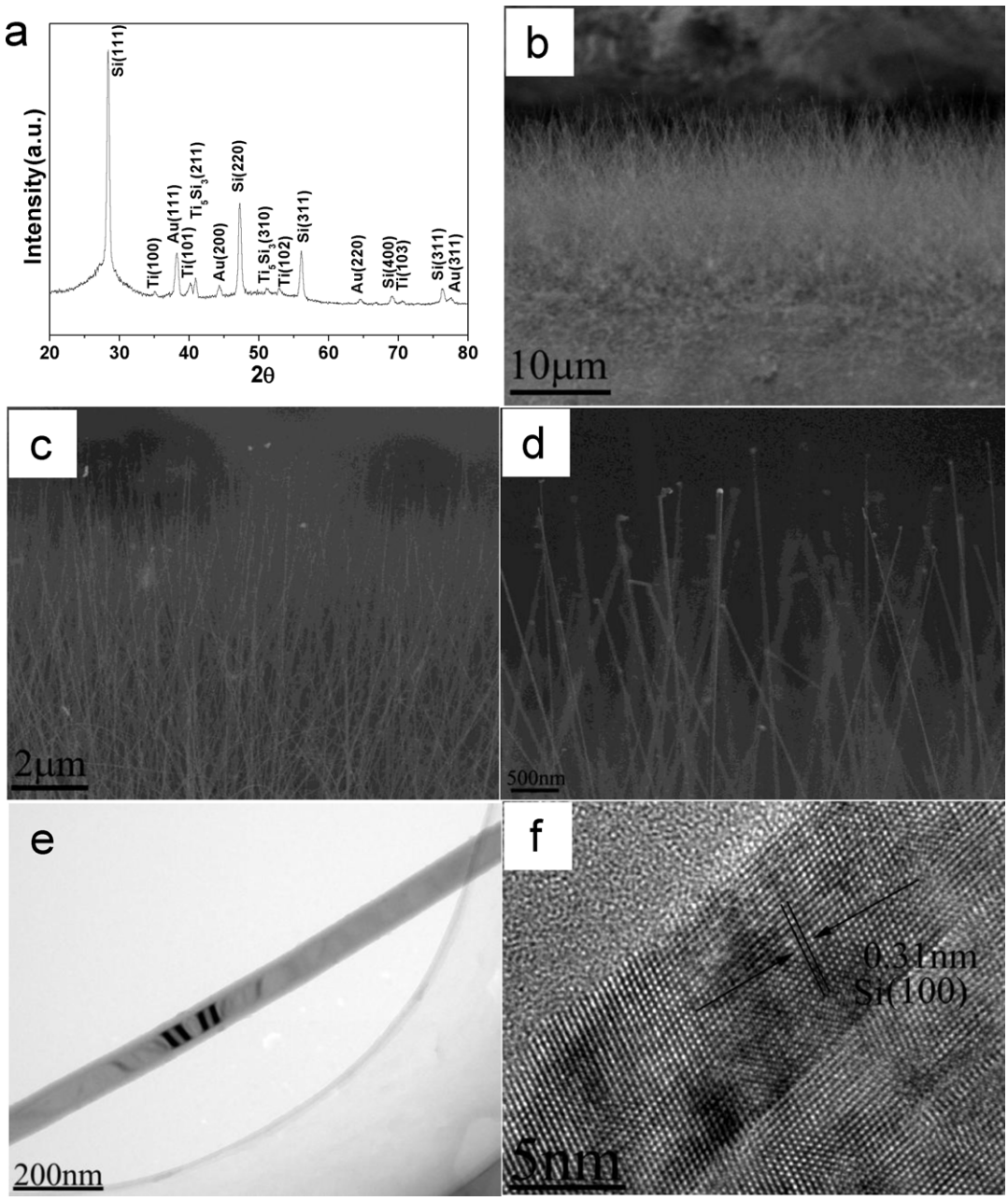

Fig. 1. Morphological and structural characterizations of the SiNA obtained by HFCVD with Au films of 5 nm as a catalyst for 1 min. (a) XRD pattern, (b–d) SEM images, (e) TEM image, and (f) HRTEM image.

indicated that the thickness of Au layer played a key role in the formation of the SiNA. We also evaluated the performance of the SiNA as anode of Li-ion batteries compared to the disordered Si nanowires.

2. Experimental

SiNA were grown on Ti substrates by a vapour-phase approach with Au film as a catalyst. In a typical synthesis, Ti substrate was firstly cleaned with 5% hydrochloric acid for 10 min, washed with deionized water, and dried in N_2. Secondly, Au film was deposited onto the Ti substrate by magnetic sputtering method. The thickness of the Au layer (5–50 nm) was simply tuned by the sputtering time. Finally, the Ti substrate was put into the chamber of HFCVD that was then pumped down to 0.5 Pa and heated to 650 °C. The mixed gases of argon (Ar), hydrogen (H_2) and silane (SiH_4) with a flow ratio of 10:2:1 were inlet the chamber. The pressure and temperature in the chamber were kept at 1000 Pa and 650 °C, respectively. The length of the SiNA was controlled by the reaction time.

The obtained samples were characterized by X-ray powder diffraction (XRD) using a Rigaku D/max-ga X-ray diffractometer with graphite monochromatized Cu Kα radiation (λ = 1.54178 Å). The morphology and structure of the samples were examined by transmission electron microscopy (TEM, JEM-200 CX, 160 kV), high-resolution transmission electron microscopy (HRTEM, JEOL JEM-2010) and field emission scanning electron microscopy (FESEM, Hitachi S-4800).

Electrochemical measurements were carried out using two-electrode coin-type cells with a lithium metal as the counter electrodes. The cell assembly was performed in a glove-box filled with pure argon (99.999%) in the presence of an oxygen scavenger and a sodium drying agent. The cells using 1 M solution of $LiPF_6$ in ethylene carbonate (EC) and dimethyl carbonate (DMC) (1:1 by vol.) as the electrolyte solution were assembled in an Ar-filled glove box (Mbraun, labstar, Germany) and each cell was aged for 12 h before the electrochemical tests. Charge–discharge cycles were tested with a current density of 0.05–1 C and in the potential range of 0.01–1.2 V.

3. Results and discussion

Fig. 1 shows the morphological and structural characterizations of the products deposited on Ti substrate by HFCVD for 1 min using Au films of 50 nm in thickness as a catalyst. As observed from XRD

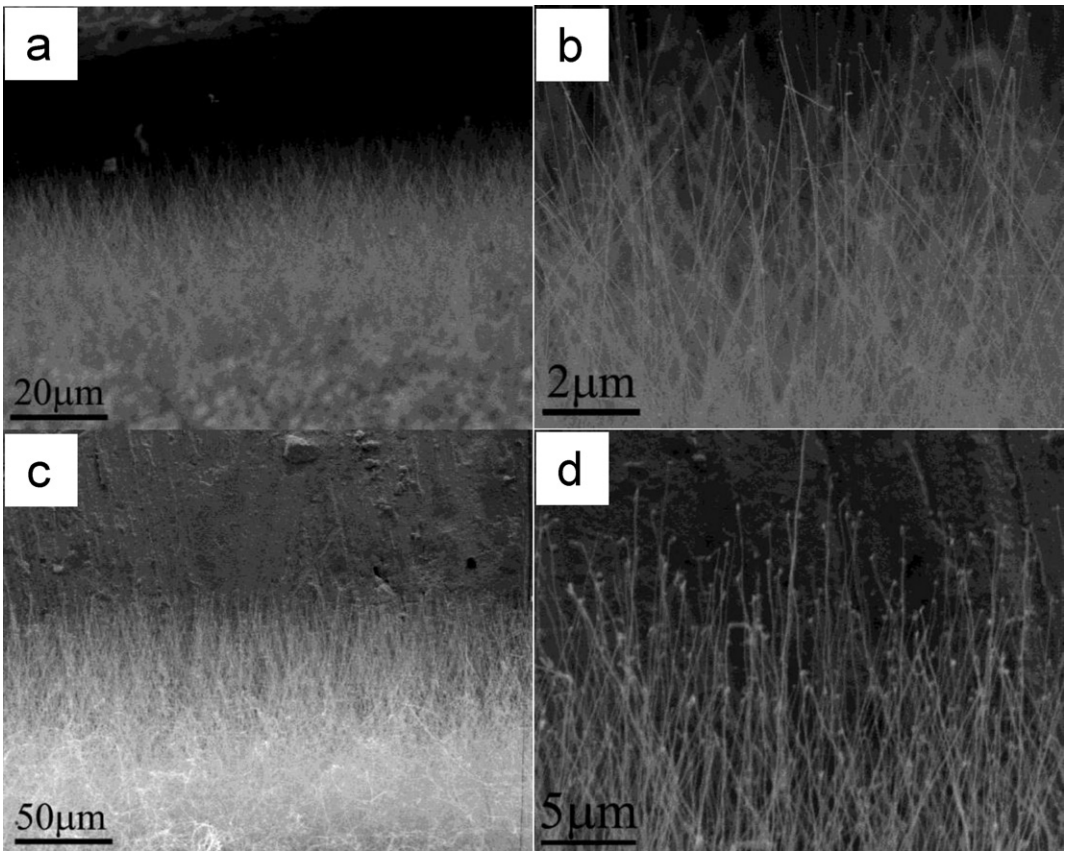

Fig. 2. SEM images of Si nanostructures prepared for different times. (a and b) 2 and (c and d) 6 min.

pattern (Fig. 1a), the peaks can be assigned to metal Ti (JCPDS Card No. 89-2762), Si (JCPDS Card No. 01-0787), Ti_5Si_3 (JCPDS Card No. 89-3721) and Au, respectively, indicating the deposition of pure Si on Ti substrate using Au as catalyst. The Ti_5Si_3 forms at the interface between the Ti substrate and the SiNA during the growth process, which could buffer the lattice mismatch and enhance the adhesion between Ti and Si, thus might benefit the charge–discharge process. The array structures of Si nanowires can be primarily verified by the SEM image (Fig. 1b), which is different from the previously reported Si nanowires with a disordered structure [33]. It should be pointed out that SiNA on Ti substrate was not as neat as that on Si substrate due to uneven surface of Ti substrate and the lattice mismatch between Si and Ti [34]. From the magnified SEM images (Fig. 1c and d), each nanowire of the SiNA was terminated by a small nanoparticle of the catalyst, indicating that the conventional vapour–liquid–solid (VLS) mechanism dominated the growth of the Si nanowires. Moreover, the lengths and diameters of the silicon nanowires were about 10 μm and 100 nm, respectively. Fig. 1e and f shows the TEM and HRTEM images of an individual Si nanowire. As observed, the Si nanowires were straight, which may support the formation of array structure. The HRTEM image clearly shows well-resolved, continuous fringes in the same orientation, indicating that the nanowire of silicon was single-crystalline in nature. The lattice spacing of 0.31 nm corresponds to the {1 0 0} plane of Si. The above characterizations confirmed the synthesis of the SiNA on Ti substrate.

The lengths of the Si nanowires were simply controlled by adjusting the reaction time. Fig. 2a and b shows the SEM image of the products obtained by prolonging the reaction time to 2 min. As observed from these images, the SiNA were obtained with a length of 20 μm. When the reaction time had proceeded to 6 min, the lengths of The SiNA increased to about 50 μm, indicating that the lengths of the SiNA could be adjusted by the reaction time.

In general, Au layer with thickness of about 5–10 nm was employed as a catalyst for effectively guiding the growth of Si nanowires via a VLS mechanism [35–37]. Herein, a thicker Au layer (50 nm) was deposited on Ti substrate and applied as the catalyst for the synthesis of the SiNA. Fig. 3a and b shows the SEM image of the Si nanowires prepared with Au layer of 20 nm in thickness. As can be seen, the disordered Si nanowires were synthesized on Ti substrate rather than the SiNA. When the thickness of Au layer decreased to 5 nm, only sparse Si nanowires were grown on Ti substrate (Fig. 3c and d). Taken together, the thickness of Au catalyst played an important role in the formation of the SiNA.

Fig. 4 illustrates a plausible mechanism responsible for the formation of the SiNA. As is well-known, the thick Au layer could be transformed to Au arrays with high-density nanoparticles on Ti substrate during the heating process. Subsequently, the newly formed Si atoms were continuously added to molten Au nanoparticles, and thus the formation of Au–Si alloyed droplets. After that, Si atoms nucleated and grew into the Si nanowires through a VLS mechanism. Two factors were expected to promote the growth of the arrayed nanostructure: (1) the dense Au nanoparticles led to the short distance between the Si nanowires in the initial growth stage. As a result, the adjacent Si nanowires could support each other, which was beneficial to the formation of the arrayed structure. (2) The growth rate of Si nanowires in HFCVD is faster than conventional CVD system due to the large temperature gradient between the growth substrate and the silane atmosphere, which may also facilitate the array structure [38].

The SiNA with a length of 10 μm (Fig. 1) and the disordered Si nanowires (Fig. 3c) were then tested as anode of Li-ion

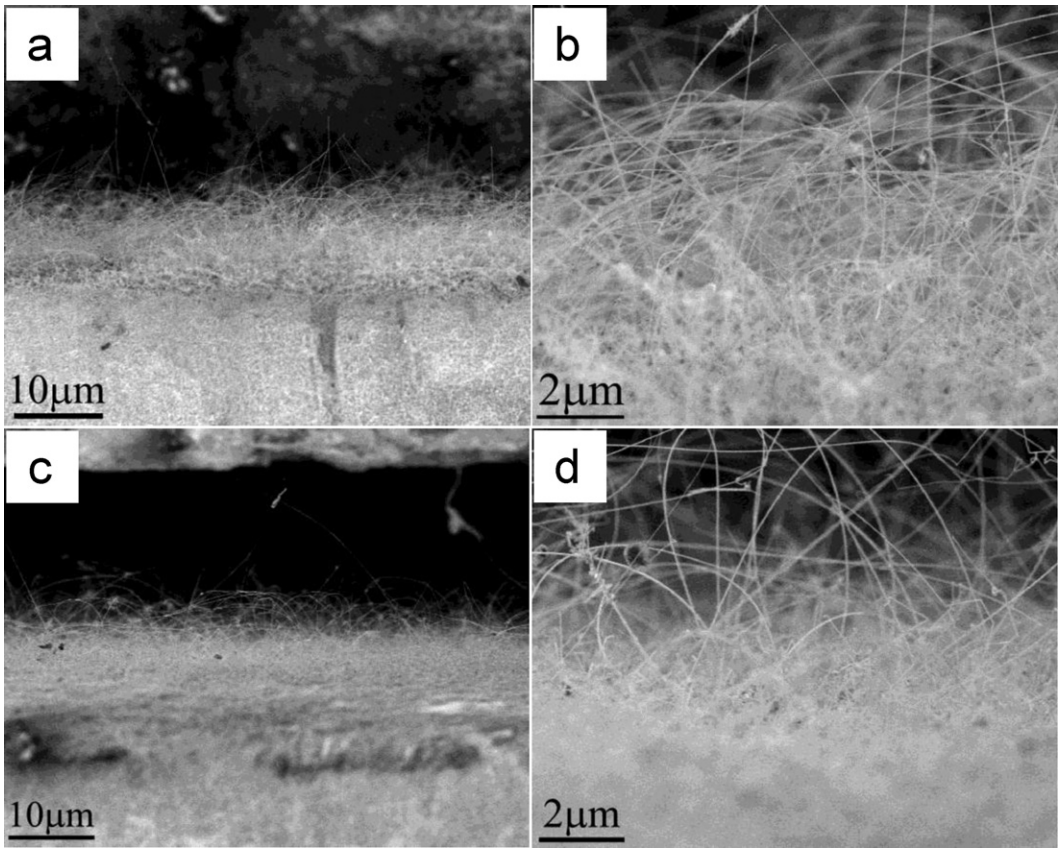

Fig. 3. SEM images of the Si nanostructures prepared using Au films with different thickness as a catalyst. (a and b) 20 and (c and d) 5 nm.

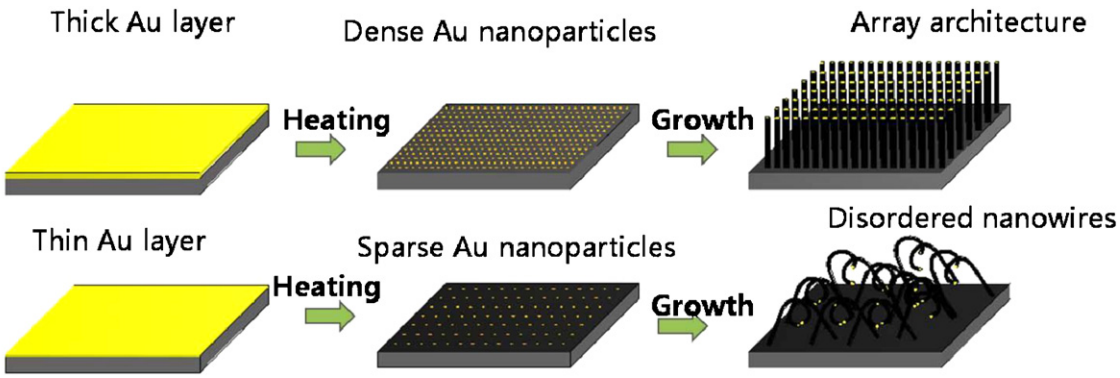

Fig. 4. Schematic illustrating a plausible mechanism for the formation of the SiNA and disordered Si nanowires obtained using Au films with different thickness as a catalyst.

batteries. Fig. 5a shows the first three cyclic voltammogram (CV) curves of the electrodes made from the SiNA at a scan rate of 0.5 mV s^{-1} and a temperature of 20 °C. During the discharge process, the peaks at 100–350 mV associated with the formation of the Li–Si alloy. Upon charge, the peaks appeared at about 370 and 610 mV, corresponded to the phase transition between amorphous Li_xSi phases, which was consistent with the previous reported [33,39,10]. The magnitude of the peaks increased with cycle due to activation of more material to react with Li in each scan [33,39]. Fig. 5b shows the 1st, 10th and 20th discharge curves of the electrodes made from the SiNA at a current density of 0.05 C. It can be seen that a long flat plateau during the first discharge corresponded to the formation of amorphous Li_xSi and subsequent discharge cycles had different voltage profiles characteristic of amorphous Si [10,40–42,6,43]. The discharge capacities of the electrode in the 1st, 10th, and 20th cycles were 3668.5, 3541.3 and 3443.6 mAh g^{-1}, respectively. The capacity after 20 cycles showed about 93.8% capacity retention, indicating the high reversible property of the SiNA as anode of Li-ion batteries. In addition, the SiNA electrodes showed about 3650, 2980, 2650 and 2200 mAh g^{-1} of discharge capacity at 0.05, 0.2, 0.5 and 1 C, respectively (Fig. 5c). The degradation (from 0.05 C to 1 C) might be resulted from low electron conductivity and lithium ion diffusivity, both of which were inherent properties of intrinsic silicon [44]. When the current density was reduced to 0.05 C again after 20 cycles, the capacity was recovered to about 3600 mAh g^{-1}. As a result, the SiNA exhibited an enhanced capacity as anode of Li-ion batteries than the previously reported Si nanowires/nanotubes [14,33,10,44–47]. From Fig. 5d, the first charging capacity was about 4245 mAh g^{-1}, which was essentially equivalent to the theoretical capacity within

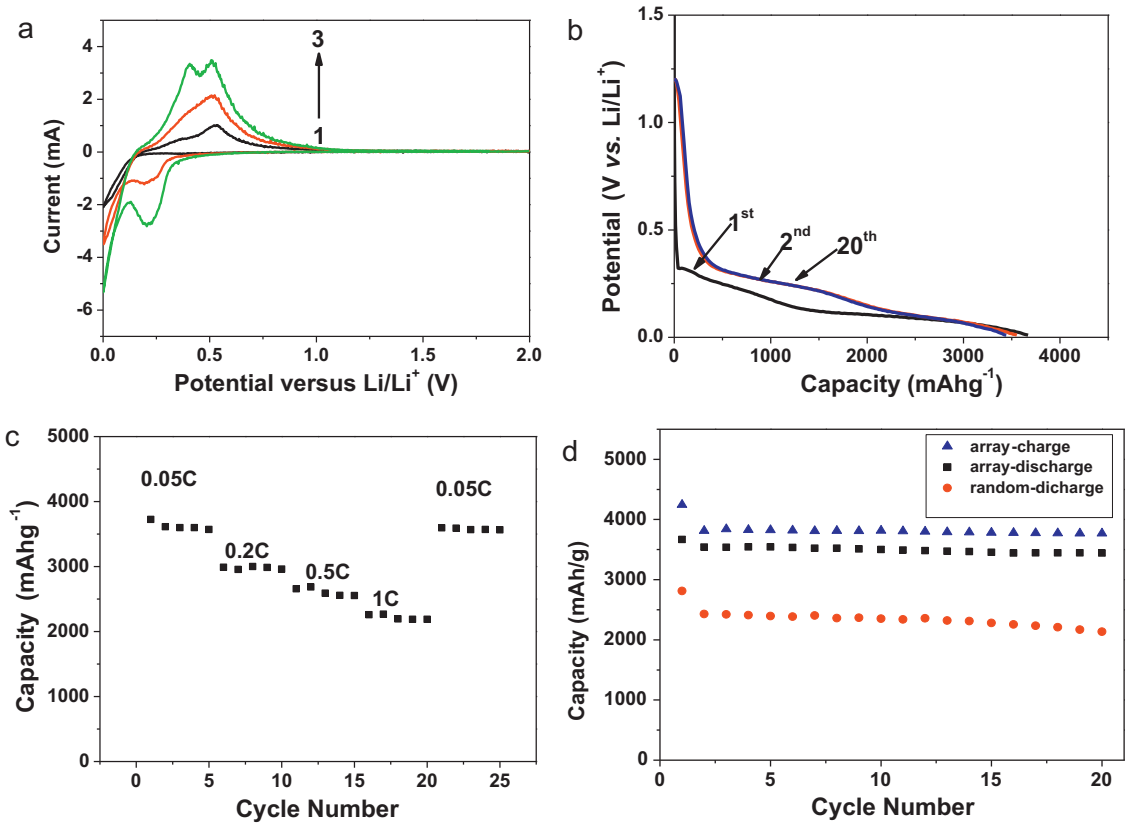

Fig. 5. (a) The first three cyclic voltammogram (CV) curves of the electrodes made of the SiNA at a scan rate of 0.5 mV s^{-1} and a temperature of 20 °C. (b) The 1st, 10th and 20th discharge curves of the electrodes made of the SiNA at a current density of 0.05 C. (c) Capabilities of the SiNA at different C rates. (d) The charge and discharge capacity for the SiNA, and the capacity for disordered Si nanowires vs. cycle number at 0.05 C.

experimental error [33]. The initial Coulombic efficiency was about 86.4%, which was much higher than that of the disordered Si nanowires. The array structure might be responsible for the higher initial Coulombic efficiency. After first cycle, the charge and discharge capacity remained the constant, with little fading up to 20 cycles. As observed, the SiNA exhibited much larger capacity and higher initial Coulombic efficiency than those of the disordered Si nanowires. The easier diffusion of electrolyte and shorter lithium ion diffusion path were supposed to be responsible for the improved performance. Furthermore, the higher density and loading of Si nanowire arrays can ease the electrodes collapse during the cycling, which may also be meaningful to the improved performance. However, the exact mechanism needed further investigation.

4. Conclusions

In summary, we have synthesized the SiNA on Ti substrate through HFCVD using Au film as a catalyst. The thickness of the Au layer played important role in controlling the morphology of Si nanowires. The thick Au layer induced the formation of the SiNA, while the thin Au layer resulted in the disordered Si nanowires. The SiNA were applied as anode of Li-ion batteries, which showed larger reversible capacity (3600 mAh g^{-1}) and higher initial Coulombic efficiency (86.4%) than those of the disordered Si nanowires and bulk Si materials. The array nanostructures can lead to the easier diffusion of electrolyte and shorter lithium ion diffusion path, which might be responsible for the improved performance. We believed that the SiNA might find potential applications in the next generation of Li-ion batteries.

Acknowledgements

The authors would like to appreciate the financial support from the 863 Project (No. 2011AA050517), NSFC (No. 51002133) and Fundamental Research Funds for the Central Universities (Program No. 2011FZA4006).

References

[1] J.M. Tarascon, M. Armand, Nature 414 (2001) 359.
[2] B.A. Boukamp, G.C. Lesh, R.A. Huggins, J. Electrochem. Soc. 725 (1981) 128.
[3] M. Winter, J.O. Besenhard, M.E. Spahr, P. Novak, Adv. Mater. 725 (1998) 10.
[4] S. Ohara, J. Suzuki, K. Sekine, T. Takamura, J. Power Sources 591 (2003) 119.
[5] L.Y. Beaulieu, T.D. Hatchard, A. Bonakdarpour, M.D. Fleischauer, J.R. Dahn, J. Electrochem. Soc. 150 (2003) A1457.
[6] T.D. Hatchard, J.R. Dahn, J. Electrochem. Soc. 151 (2004) A838.
[7] H. Kim, M. Seo, M.-H. Park, J. Cho, Angew. Chem. Int. Ed. 49 (2010) 2146.
[8] M.-H. Park, M.G. Kim, J. Joo, K. Kim, J. Kim, S. Ahn, Y. Cui, J. Cho, Nano Lett. 9 (2009) 3844.
[9] T. Song, J.L. Xia, J.-H. Lee, D.H. Lee, M.S. Kwon, J.-M. Choi, J. Wu, S.K. Doo, H. Chang, W.I. Park, D.S. Zang, H. Kim, Y.G. Huang, K.-C. Hwang, J.A. Rogers, U. Paik, Nano Lett. 10 (2010) 1710.
[10] H. Kim, J. Cho, Nano Lett. 8 (2008) 3688.
[11] L.F. Cui, R. Ruffo, C.K. Chan, H.L. Peng, Y. Cui, Nano Lett. 9 (2009) 491.
[12] L.F. Cui, Y. Yang, C.-M. Hsu, Y. Cui, Nano Lett. 9 (2009) 3370.
[13] R. Teki, M. Datta, R. Krishnan, T. Parker, T. Lu, P. Kumta, N. Koratkar, Small 5 (2009) 2236.
[14] H. Nguyen, F. Yao, M. Zamfir, C. Biswas, K. So, Y. Lee, S. Kim, S. Cha, J. Kim, D. Pribat, Adv. Energy Mater. 1 (2011) 1154.
[15] M. Au, Y. He, Y. Zhao, H. Ghassemi, R. Yassar, B. Garcia-Diaz, T. Adams, J. Power Sources 196 (2011) 9640.
[16] W. Xu, S. Vegunta, J. Flake, J. Power Sources 196 (2011) 8583.
[17] S. Chou, Y. Zhao, J. Wang, Z. Chen, H. Liu, S. Dou, J. Phys. Chem. C 114 (2010) 15862.
[18] R. Lv, J. Yang, P. Gao, Y. NuLi, J. Wang, J. Alloys Compd. 490 (2010) 84.
[19] X. Yang, Z. Wen, L. Zhang, M. You, J. Alloys Compd. 464 (2008) 265.
[20] G. Che, K.B. Jirage, E.R. Fisher, C.R. Martin, J. Electrochem. Soc. 144 (1997) 4296.

[21] M. Nishizawa, K. Mukai, S. Kuwabata, C.R. Martin, H. Yoneyama, J. Electrochem. Soc. 144 (1997) 1923.
[22] G. Che, B.B. Lakshmi, E.R. Fisher, C.R. Martin, Nature 393 (1998) 346.
[23] N. Li, C.J. Patrissi, G. Che, C.R. Martin, J. Electrochem. Soc. 147 (2000) 2044.
[24] N. Li, C.R. Martin, J. Electrochem. Soc. 148 (2001) A164.
[25] C.J. Patriss, C.R. Martin, J. Electrochem. Soc. 148 (2001) A1247.
[26] C.R. Sides, C.R. Martin, Adv. Mater. 17 (2005) 125.
[27] P.L. Taberna, S. Mitra, P. Poizot, P. Simon, J.M. Tarascon, Nat. Mater. 5 (2006) 567.
[28] J. Hassoun, S. Panero, P. Simon, P.L. Taberna, B. Scrosati, Adv. Mater. 19 (2007) 1632.
[29] Y.G. Li, B. Tan, Y.Y. Wu, Nano Lett. 8 (2008) 265.
[30] J.P. Liu, Y.Y. Li, X.T. Huang, R.M. Ding, Y.Y. Hu, J. Jiang, L. Liao, J. Mater. Chem. 19 (2009) 1859.
[31] D. Fang, K. Huang, S. Liu, Z. Li, J. Alloys Compd. 464 (2008) L5.
[32] Z. Wu, L. Qin, Q. Pan, J. Alloys Compd. 509 (2011) 9207.
[33] C.K. Chan, H.L. Peng, G. Liu, K. Mcilweath, X.F. Zhang, R.A. Huggins, Y. Cui, Nat. Nanotechnol. 3 (2008) 31.
[34] A.I. Hochbaum, R. Fan, R.R. He, P.D. Yang, Nano Lett. 5 (2005) 457.
[35] J. Westwater, D.P. Gosain, S. Tomiya, S. Usui, J. Vac. Sci. Technol. B15 (1997) 554.
[36] F.M. Kolb, H. Hofmeister, R. Scholz, M. Zacharias, U. Gösele, D.D. Ma, S.T. Lee, J. Electrochem. Soc. 151 (2004) G472.
[37] S. Sharama, T.I. Kamins, R.S. Williams, Appl. Phys. A 80 (2005) 1225.
[38] Y. Yao, F.H. Li, S.-T. Lee, Chem. Phys. Lett. 406 (2005) 381.
[39] M. Green, E. Fielder, B. Scrosati, M. Wachtler, J.S. Moreno, Electrochem. Solid-State Lett. 6 (2003) A75.
[40] A. Netz, R.A. Huggins, W. Weppner, J. Power Sources 119–121 (2003) 95.
[41] J. Li, J.R. Dahn, J. Electrochem. Soc. 154 (2007) A156.
[42] M.N. Obrovac, L.J. Krause, J. Electrochem. Soc. 154 (2007) A103.
[43] H. Li, F. Cheng, Z. Zhu, H. Bai, Z. Tao, J. Chen, J. Alloys Compd. 509 (2011) 2919.
[44] T. Song, J.L. Xia, J.-H. Lee, D.H. Lee, M.-S. Kwon, J.-M. Choi, J. Wu, S.K. Doo, H. Chang, W.I. Park, D.S. Zang, H. Kim, Y.G. Huang, K.-C. Hwang, J.A. Rogers, U. Paik, Nano Lett. 10 (2010) 1710.
[45] L.-F. Cui, Y. Yang, C.-M. Hsu, Y. Cui, Nano Lett. 9 (2009) 3370.
[46] L.-F. Cui, R. Ruffo, C.K. Chan, H.L. Peng, Y. Cui, Nano Lett. 9 (2009) 491.
[47] K.Q. Peng, J.S. Jie, W.J. Zhang, S.-T. Lee, Appl. Phys. Lett. 93 (2008) 033105.